2013 American Control Conference (ACC)
Washington, DC, USA, June 17-19, 2013

Iteratively Learning the $\mathcal{H}_\infty$-Norm of Multivariable Systems Applied to Model-Error-Modeling of a Vibration Isolation System

Tom Oomen, Rick van der Maas, Cristian R. Rojas, and Håkan Hjalmarsson

***Abstract*— The aim of this paper is to develop a new data-driven approach for learning the $\mathcal{H}_\infty$-norm of multivariable systems that can be used for model-error-modeling in robust feedback control. The proposed algorithm only requires iterative experiments on the system. Especially for the multivariable situation that is considered in this paper, these experiments have to be judiciously chosen. The proposed algorithm delivers an estimate of the $\mathcal{H}_\infty$-norm of an unknown multivariable system, without the need or explicit construction of a (parametric or non-parametric) model. The results are experimentally demonstrated on model-error-modeling of a multivariable industrial active vibration isolation system. Finally, connections to learning control algorithms are established.**

I. Introduction

Iterative approaches, including iterative learning control (ILC) [1], [2], [3], [4], and iterative identification and control [5], have received significant research attention and many successful applications have been reported. Typically, such algorithms enhance the performance of control systems.

Recently in [6, Sec. 12.2], a data-driven iterative procedure is proposed that enables a direct estimation of the $\mathcal{H}_\infty$-norm for single-input single-output (SISO) systems. A typical application of such an iterative algorithm is in model error modeling, since many reliable robust control design methodologies consider model errors as $\mathcal{H}_\infty$-norm bounded perturbations. In [7], the data-driven iterative $\mathcal{H}_\infty$-norm estimation is extended, followed by a thorough stochastic analysis in [8]. In [9], the procedure is successfully applied for robust stability analysis of a SISO experimental setup.

Although the iterative $\mathcal{H}_\infty$-norm estimation algorithm in [6], [7], [8] is potentially very useful for model error modeling, its limitation to SISO systems prohibits its application for many relevant applications that often have multiple inputs and outputs. Unfortunately, the approach for SISO systems, which relies on a judicious application of time reversal operators, cannot be directly extended to multi-input multi-output (MIMO) systems. This paper aims to extend iterative $\mathcal{H}_\infty$-norm estimation towards multivariable systems.

The main contribution of this paper is an iterative data-driven multivariable $\mathcal{H}_\infty$-norm estimation procedure. This procedure delivers an estimate of the $\mathcal{H}_\infty$-norm of a multivariable system without the use of a (parametric or non-parametric) model. The derivation of the procedure relies heavily on finite time representations of the multivariable system as in [10] and [11], in conjunction with a well-established algorithm in matrix computations [12]. The procedure is experimentally verified for model error modeling of an active vibration isolation system (AVIS). Such systems are used to isolate highly accurate systems from external disturbances in multiple degrees-of-freedom through the application of skyhook damping, see [13]. In addition to the use of time reversal operators as in the SISO case [6], [7], [8], the multivariable situation requires a delicate derivation, which is essentially due to the fact that multivariable systems in general do not commute.

This paper is organized as follows. In Sec. II, contains the problem definition. Then, in Sec. III, a new data-driven multivariable $\mathcal{H}_\infty$-norm estimation algorithm is presented. Sec. IV contains an experimental verification of the proposed algorithm. Finally, a discussion and a conclusion are provided in Sec. V and Sec. VI, respectively.

II. Motivation and problem formulation

The aim of this paper is to present a novel procedure that enables estimation of the $\mathcal{H}_\infty$-norm γ of a certain transfer function matrix $\Delta_o \in \mathcal{RH}_\infty^{p\times q}$. The motivation for considering this problem stems from model error modeling, where a true system P_o and a model $\hat{P}$ are given. In the case of an additive perturbation structure (see [14] for an appropriate definition) the model error Δ_o is given by

$$\Delta_o = \hat{P} - P_o. \tag{1}$$

If the model uncertainties are represented as $\mathcal{H}_\infty$-norm bounded perturbations, i.e., perturbations in the class

$$\mathbf{\Delta}_u := \{\Delta_u | \|\Delta_u\|_\infty \leq \gamma\}$$

are considered. The main rationale is that if a feedback system is robust with respect to perturbations in $\mathbf{\Delta}_u$, then it is robust with respect to the model error Δ_o with $\|\Delta_o\|_\infty \leq \gamma$. Hence, accurate estimation of γ is of vital importance for robustness analysis and robust controller synthesis.

The considered problem considered in this paper is to directly estimate the size γ of Δ_o based on measured data, hence without resorting to an intermediate step of (parametric or non-parametric) modeling. In contrast, the approach in [15] involves the estimation of an auxiliary model of the model error Δ_o, whereas [16] and [17] employ a nonparametric model, i.e., an identified frequency response function, of Δ_o. In these approaches, the identified model is subsequently used to compute the $\mathcal{H}_\infty$ norm.

The pursued approach to estimate γ is to perform experiments on Δ_o. Hereto, the input u_Δ is applied to Δ_o and

T. Oomen and R. van der Maas are with the Eindhoven University of Technology, Department of Mechanical Engineering, Control Systems Technology Group, The Netherlands. t.a.e.oomen@tue.nl. C. Rojas and H. Hjalmarsson are with the Automatic Control Lab and ACCESS Linnaeus Center, Electrical Engineering, KTH - Royal Institute of Technology, Stockholm, Sweden.

978-1-4799-0176-0/$31.00 ©2013 AACC

the output $y_\Delta = \Delta_o u_\Delta$ is measured. Note that in general experimentation on Δ_o involves both an experiment on the true system P_o and a simulation with the model $\hat{P}$. For instance, in the case of (1), $y_\Delta = \Delta_o u_\Delta = \hat{P}u_\Delta - P_o u_\Delta$. The main idea is to then directly estimate γ from y_Δ and u_Δ. In the next section, the basic procedure is presented that renders the auxiliary model estimation step superfluous. However, this requires a judicious design of the input u_Δ.

III. A DATA-DRIVEN APPROACH TO MULTIVARIABLE UNCERTAINTY MODELING

A. Iterative data-driven $\mathcal{H}_\infty$-norm estimation: SISO systems

In this section the basic principle for data-driven $\mathcal{H}_\infty$-norm estimation of SISO systems, as is also described in [8], [18], is presented. To introduce the mechanism, assume first that Δ is SISO and linear time invariant (LTI), where the subscript o is dropped for notational reasons. Notice that the $\mathcal{H}_\infty$-norm is an induced norm, i.e.,

$$\|\Delta\|_\infty = \|\Delta\|_{i2} = \sup_{u_\Delta \in \ell_2 \setminus 0} \frac{\|y_\Delta\|_2}{\|u_\Delta\|_2},$$

see [14, Sec. 4.5] for a proof. Assume that the signals have finite length $N \in \mathbb{N}$, i.e., $\underline{u_\Delta}, \underline{y_\Delta} \in \mathbb{R}^{N\times 1}$, hence

$$\|\underline{\Delta}\|_{i2} = \sup_{\underline{u_\Delta} \in \mathbb{R}^{N\times 1} \setminus 0} \frac{\|\underline{y_\Delta}\|_2}{\|\underline{u_\Delta}\|_2}. \tag{2}$$

Note that $\|\underline{\Delta}\|_{i2} \to \|\Delta\|_\infty$ for $N \to \infty$, see [8] for a proof. Next, on the finite time interval of length N,

$$\underline{y_\Delta} = \underline{\Delta}\,\underline{u_\Delta},$$

where no measurement noise is assumed and

$$\underline{\Delta} = \begin{bmatrix} r_0 & 0 & 0 & \dots & 0 \\ r_1 & r_0 & 0 & & 0 \\ \vdots & \vdots & & \ddots & 0 \\ r_{N-1} & r_{N-2} & r_{N-3} & \dots & r_0 \end{bmatrix}.$$

As a result, (2) is equivalent to

$$\begin{aligned} \|\underline{\Delta}\|_{i2} &= \sup_{\underline{u_\Delta} \in \mathbb{R}^{N\times 1} \setminus 0} \sqrt{\frac{\underline{y_\Delta}^T \underline{y_\Delta}}{\underline{u_\Delta}^T \underline{u_\Delta}}} \\ &= \sup_{\underline{u_\Delta} \in \mathbb{R}^{N\times 1} \setminus 0} \sqrt{\frac{\underline{u_\Delta}^T \underline{\Delta}^T \underline{\Delta}\,\underline{u_\Delta}}{\underline{u_\Delta}^T \underline{u_\Delta}}} = \sqrt{\lambda^{\max}(\underline{\Delta}^T \underline{\Delta})} \end{aligned} \tag{3}$$

Now, observe that

$$\underline{\Delta}^T = \mathcal{T}_N \underline{\Delta} \mathcal{T}_N, \tag{4}$$

where

$$\mathcal{T}_N = \begin{bmatrix} 0 & \dots & 0 & 1 \\ 0 & \dots & 1 & 0 \\ \vdots & & & \vdots \\ 1 & \dots & 0 & 0 \end{bmatrix},$$

i.e., $\mathcal{T}_N$ is an involutory permutation matrix of size $N \times N$. The matrix $\mathcal{T}_N$ can be given the interpretation of a time-reversal operator. Next, (4) reveals that $\mathcal{T}_N \underline{\Delta}$ is symmetric, hence

$$\|\underline{\Delta}\|_{i2} = \lambda^{\max}(\mathcal{T}_N \underline{\Delta}). \tag{5}$$

As a result, $\|\underline{\Delta}\|_{i2}$ equals the largest eigenvalue of the matrix $\mathcal{T}_N \underline{\Delta}$. Therefore, given the impulse response r_i, $i = 1, \dots, N$, $\|\underline{\Delta}\|_{i2}$ can be directly computed through an eigenvalue analysis. In contrast, in this paper another approach is pursued to determine $\|\underline{\Delta}\|_{i2}$ that does not require knowledge of r_i, $i = 1, \dots, N$.

The following procedure enables the computation of $\|\underline{\Delta}\|_{i2}$ without requiring knowledge of r_i, $i = 1, \dots, N$.

Procedure 1 (SISO $\|\underline{\Delta}\|_{i2}$ estimation): Perform the following sequence of steps.

1) set $n = 1$ and initialize with arbitrary $\underline{u_\Delta}^{(1)} \in \mathbb{R}^{N\times 1}$, $\underline{u_\Delta}^{(1)} \neq 0$.
2) determine $\underline{y_\Delta}^{(n)} = \underline{\Delta}\,\underline{u_\Delta}^{(n)}$.
3) time-reverse: $\underline{x_\Delta}^{(n)} = \mathcal{T}_N \underline{y_\Delta}^{(n)}$.
4) set $\underline{u_\Delta}^{(n+1)} = \underline{x_\Delta}^{(n)}$.
5) set $n \mapsto n+1$ and repeat from Step 2 until a stopping criterion is met.

Procedure 1 coincides with the power method [12, Sec. 7.3.1], which is an iterative algorithm to determine the maximal eigenvalue of a matrix. As a result, it is well-known that the estimator

$$\hat{\gamma}_1^{(n)} = \frac{\left(\underline{u_\Delta}^{(n)}\right)^T \underline{x_\Delta}^{(n)}}{\left(\underline{u_\Delta}^{(n)}\right)^T \underline{u_\Delta}^{(n)}} \tag{6}$$

converges under mild conditions to $\|\underline{\Delta}\|_{i2}$, i.e., $\hat{\gamma}_1^{(n)} \to \lambda^{\max}(\mathcal{T}_N \underline{\Delta})$ for $n \to \infty$.

Essentially, two approaches can be pursued to complete Step 2 in Procedure 1. On one hand, $\underline{\Delta}^{(n)} \underline{u_\Delta}^{(n)}$ can be evaluated on a model using impulse response coefficients r_i, $i = 1, \dots, N$. On other hand, the approach taken in this paper is to perform an experiment of length N on the true system Δ_o to evaluate $\underline{\Delta}^{(n)} \underline{u_\Delta}^{(n)}$. As a result, Procedure 1 does not need any structural knowledge of Δ_o to determine its $\mathcal{H}_\infty$-norm.

Summarizing, the iterative procedure 1 leads to an estimate $\hat{\gamma}_1^{(n)}$ of $\|\Delta_o\|_\infty$ for a sufficiently large number of iterations n and sufficiently long experiment length N. Herein, each iteration requires one experiment of length N on the true system Δ_o, provided that Δ_o is SISO. In the next section, the estimation of the $\mathcal{H}_\infty$-norm of MIMO systems is investigated.

B. Data-driven $\mathcal{H}_\infty$-norm estimation of MIMO systems

In this section, a novel procedure for $\mathcal{H}_\infty$ estimation of MIMO systems is presented. Indeed, Procedure 1 does not directly apply to general MIMO systems for which (4) is not valid. Hence, MIMO systems introduce a significant complication compared to the SISO case in Sec. III-A.

To develop a data-driven $\mathcal{H}_\infty$-norm estimator for MIMO systems, consider the transfer function matrix of the MIMO system Δ with p outputs and q inputs:

$$\Delta = \begin{bmatrix} \Delta_{11} & \dots & \Delta_{1q} \\ \vdots & \ddots & \vdots \\ \Delta_{p1} & \dots & \Delta_{pq} \end{bmatrix} \in \mathcal{RH}_\infty^{p\times q}$$

with finite time representation for experiment length N

$$\underbrace{\begin{bmatrix} y_{\Delta 1} \\ \vdots \\ y_{\Delta p} \end{bmatrix}}_{=:\underline{y}_\Delta} = \underbrace{\begin{bmatrix} \underline{\Delta}_{11} & \cdots & \underline{\Delta}_{1q} \\ \vdots & \ddots & \vdots \\ \underline{\Delta}_{p1} & \cdots & \underline{\Delta}_{pq} \end{bmatrix}}_{=:\underline{\Delta}} \underbrace{\begin{bmatrix} u_{\Delta 1} \\ \vdots \\ u_{\Delta q} \end{bmatrix}}_{=:\underline{u}_\Delta}, \tag{7}$$

where $\underline{u_{\Delta i}} \in \mathbb{R}^{N\times 1}$, $i = 1, \ldots, q$ and $\underline{y_{\Delta i}} \in \mathbb{R}^{N\times 1}$, $i = 1, \ldots, p$. In addition, $\underline{\Delta} \in \mathbb{R}^{pN\times qN}$.

To proceed, observe that (3) is also valid for the multivariable system (7). Next, note that

$$\underline{\Delta}^T = \underbrace{\begin{bmatrix} \mathcal{T}_N & & 0 \\ & \ddots & \\ 0 & & \mathcal{T}_N \end{bmatrix}}_{=:\mathcal{T}_{qN}} \underbrace{\begin{bmatrix} \underline{\Delta}_{11} & \cdots & \underline{\Delta}_{p1} \\ \vdots & \ddots & \vdots \\ \underline{\Delta}_{1q} & \cdots & \underline{\Delta}_{pq} \end{bmatrix}}_{=:\widetilde{\underline{\Delta}}} \underbrace{\begin{bmatrix} \mathcal{T}_N & & 0 \\ & \ddots & \\ 0 & & \mathcal{T}_N \end{bmatrix}}_{=:\mathcal{T}_{pN}}, \tag{8}$$

where $\widetilde{\underline{\Delta}}$ is the finite time representation of the transfer function matrix

$$\widetilde{\Delta} = \begin{bmatrix} \Delta_{11} & \cdots & \Delta_{p1} \\ \vdots & \ddots & \vdots \\ \Delta_{1q} & \cdots & \Delta_{pq} \end{bmatrix}. \tag{9}$$

In general, $\widetilde{\Delta} \neq \Delta$. As a result, an analogous step from (3) to (5) can in principle only be made in the restrictive case where $\widetilde{\Delta} = \Delta$, i.e., if the system is symmetric.

The key step in the forthcoming developments is the observation that

$$\widetilde{\Delta} = \sum_{i=1}^{q} \sum_{j=1}^{p} \mathcal{I}_{ij} \Delta \mathcal{I}_{ij}, \tag{10}$$

where

$$\mathcal{I}_{ij} = \begin{bmatrix} 0 & \cdots & 0 & \cdots & 0 \\ \vdots & \ddots & & \ddots & 0 \\ 0 & \cdots & 1 & \cdots & 0 \\ \vdots & \ddots & & \ddots & \vdots \\ 0 & \cdots & 0 & \cdots & 0 \end{bmatrix} \in \mathbb{R}^{q\times p}$$

and the 1 is on the $(i,j)^{\text{th}}$ location.

To derive the finite time equivalent of (10), notice that the finite time representation of $\mathcal{I}_{ij}$ is given by

$$\underline{\mathcal{I}}_{ij} = \begin{bmatrix} 0 & \cdots & 0 & \cdots & 0 \\ \vdots & \ddots & & \ddots & 0 \\ 0 & \cdots & I_N & \cdots & 0 \\ \vdots & \ddots & & \ddots & \vdots \\ 0 & \cdots & 0 & \cdots & 0 \end{bmatrix} \in \mathbb{R}^{qN\times pN},$$

where $\underline{\mathcal{I}}_{ij}$ is a block-diagonal matrix of $q \times p$ blocks of dimension $N \times N$. Herein, the $(i,j)^{\text{th}}$ block-element is equal to an identity matrix of size N. Next,

$$\widetilde{\underline{\Delta}} = \sum_{i=1}^{q} \sum_{j=1}^{p} \underline{\mathcal{I}}_{ij} \underline{\Delta} \underline{\mathcal{I}}_{ij}. \tag{11}$$

The result (11) is the basis for the following procedure, which constitutes the main contribution of this paper.

Procedure 2 (MIMO $\|\underline{\Delta}\|_{i2}$ estimation): Perform the following sequence of steps.

1) set $n = 1$ and initialize with arbitrary $\underline{u_\Delta}^{(1)} \in \mathbb{R}^{qN\times 1}$, $\underline{u_\Delta}^{(1)} \neq 0$.

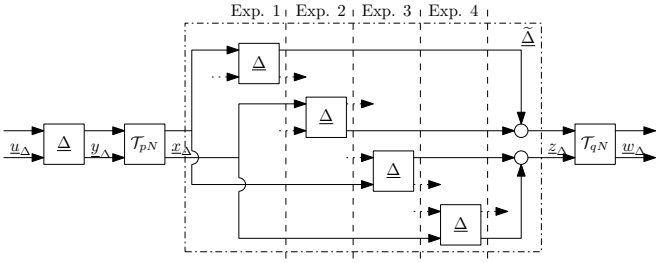

Fig. 1. Illustration of one iteration n of Procedure 2 for $p = q = 2$. The disconnected inputs are taken equal to zero.

2) determine $\underline{y_\Delta}^{(n)} = \underline{\Delta}\,\underline{u_\Delta}^{(n)}$.
3) time-reverse: $\underline{x_\Delta}^{(n)} = \mathcal{T}_{pN}\underline{y_\Delta}^{(n)}$.
4) set $\underline{z_\Delta}^{(n)} = 0$ and perform pq experiments:

```
for i = 1, ..., q
      for j = 1, ..., p
       z_Δ^(n) ↦ z_Δ^(n) + I_ij Δ I_ij x_Δ^(n)
      end
end
```

5) time reverse: $\underline{w_\Delta}^{(n)} = \mathcal{T}_{qN}\underline{z_\Delta}^{(n)}$.
6) set $\underline{u_\Delta}^{(n+1)} = \underline{w_\Delta}^{(n)}$.
7) set $n \mapsto n + 1$ and repeat from Step 2 until a stopping criterion is met.

The multivariable $\mathcal{H}_\infty$-norm can subsequently be estimated from

$$\hat{\gamma}_2^{(n)} = \sqrt{\frac{\left(\underline{u_\Delta}^{(n)}\right)^T \underline{w_\Delta}^{(n)}}{\left(\underline{u_\Delta}^{(n)}\right)^T \underline{u_\Delta}^{(n)}}}, \tag{12}$$

where in contrast to Procedure 1, a square root appears due to the fact that the reduction from two experiments to 1 per step in the SISO procedure (based on (3) to (5)) is not made in the derivation of Procedure 2.

Basically, (10) and Procedure 2 recast the evaluation of $\underline{\Delta}^T$ as $p \cdot q$ experiments on $\underline{\Delta}$, for which the true system Δ_o is accessible. Hence, the approach does not require explicit knowledge of $\underline{\Delta}^T$ and $\underline{\Delta}$. This is enabled by linearity, since (10) exploits superposition. A single iteration of the proposed procedure 2 applied to a two input two output MIMO system is illustrated in Fig. 1.

C. Convergence and implementation aspects

Importantly, the algorithms in Procedure 1 and Procedure 2 are globally convergent. This follows directly from the observation that these procedures can be related to the power iterations method for computing the largest eigenvalue of a matrix, see [12, Sec. 8.2]. In addition, it should be remarked that the finite time induced 2-norm in (2) converges to the $\mathcal{H}_\infty$-norm for $N \to \infty$, see [8, Theorem 3] for a proof.

The actual implementation on physical systems of the data-driven $\mathcal{H}_\infty$-norm estimation procedures 1 and 2 for SISO and MIMO systems, respectively, requires some additional attention. First, the input $\underline{u_\Delta}^{(n)}$ to the system Δ_o is usually subject to constraints, including energy, power, and amplitude constraints. These can directly be dealt with.

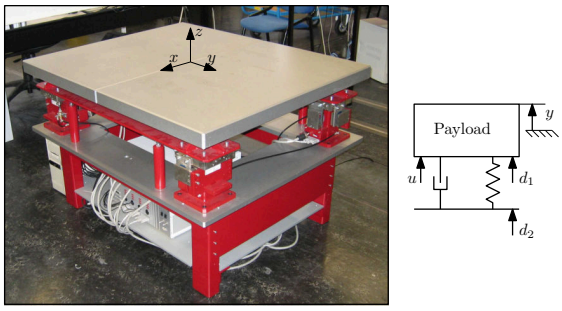

Fig. 2. Picture and schematic illustration of AVIS. The rotation around the x-axis is denoted by ϕ.

Hereto, let the input

$$\frac{1}{\mu^{(n)}}\underline{u_\Delta}^{(n)} \tag{13}$$

satisfy the input constraints and apply it to the system Δ_o. Then, by linearity, $\mu^{(n)}\Delta_o\frac{1}{\mu^{(n)}}\underline{u_\Delta}^{(n)} = \Delta_o\underline{u_\Delta}^{(n)}$. Hence, either the output of Δ_o should be scaled by $\mu^{(n)}$ or the estimators $\hat{\gamma}_1$ and $\hat{\gamma}_2$ should be appropriately extended with the reciprocal of the input normalization $\frac{1}{\mu^{(n)}}$, i.e., $\mu^{(n)}$.

Second, physical systems are generally subject to unmeasured disturbances. Recently, in [18], [8], it has been shown that these may lead to a bias error of the estimator $\hat{\gamma}_1^{(n)}$. However, the bias error for the considered system can be made sufficiently small. Indeed, the input can be made sufficiently large while satisfying the input signal constraints.

IV. Experimental results

A. Description of industrial AVIS

The AVIS in Fig. 2 is considered in this paper. The system consists of two main parts, i.e., a movable payload and a chassis that is connected to the floor. The payload and chassis are interconnected through four isolator modules. On one hand, these isolator modules provide passive damping through a pneumatic airmount. On the other hand, the isolator models are equipped with Lorentz motors and geophones that enable active vibration isolation through skyhook damping that exploits the absolute velocity measurements [13].

A nominal model $\hat{P}$ of the AVIS system has already been identified. In this paper, attention is restricted to a 2 input, 2 output subsystem in z-translation and ϕ-rotation. In Fig. 3, the parametric model $\hat{P}$ and nonparametric frequency response function of the model P_o are depicted. After the selection of a suitable uncertainty structure, the inputs and outputs of the model error $\Delta_o \in \mathcal{RH}_\infty^{2\times 2}$ are accessible. This follows similarly as the example of an additive structure in (1). In the next section, the norm γ of the model error Δ_o is determined through the iterative Procedure 2.

To obtain an idea of the shape of Δ_o, the frequency response function of Δ_o is identified. Hereto, the frequency response identification approach in [19] is employed, see Fig. 4 for the results. It is emphasized that the resulting frequency response function of Δ_o is not required for using the power iterations algorithm in Sec. III. However, it does

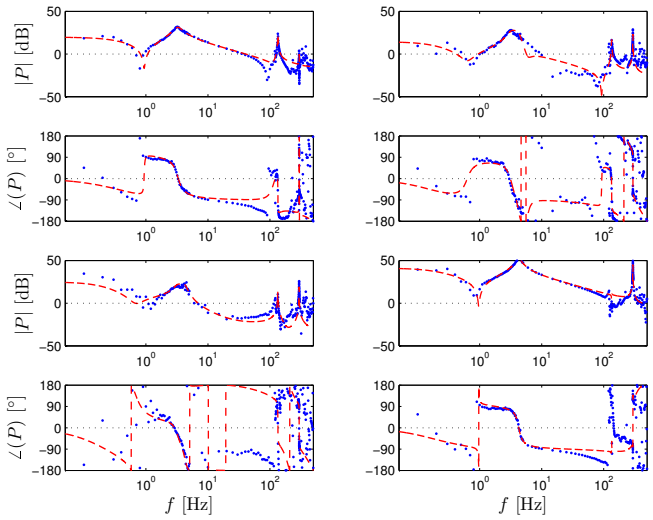

Fig. 3. Nonparametric frequency response function P_o (blue dots) and identified parametric model $\hat{P}$ (dashed red). Both the z-translation and ϕ-rotation are displayed.

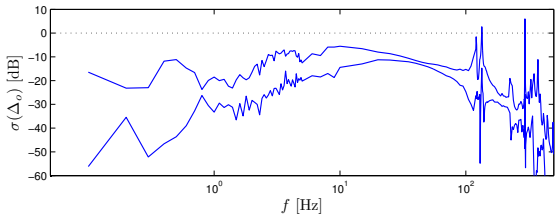

Fig. 4. Frequency response function estimate of Δ_o.

provide insight into the shape of Δ_o and a reference value for γ. In particular, the peak value of $\bar{\sigma}(\Delta_u)$ over frequency equals 1.95, which is attained at a frequency of 296 [Hz]. Notice that a rather dense frequency grid has been employed to determine the frequency response function Δ_o, leading to a fairly long experimentation time.

In the next section, Algorithm 2 is applied to estimate γ.

B. Data-driven $\mathcal{H}_\infty$-norm estimation of the multivariable AVIS model error

In this section, the data-driven $\mathcal{H}_\infty$-norm estimation procedure presented in Sec. III-B is applied to the AVIS system in Sec. IV-A. In particular, the z-translation and ϕ-rotation in Fig. 2 are considered.

In this section, the key experimental results of this paper are presented, which involve the application of Procedure 2 in view of uncertainty modeling of the AVIS.

The application of Procedure 2 leads to the following observations.

1) The iteration is initialized with $\underline{u_\Delta}^{(1)}$ being zero mean white noise, see Fig. 5.
2) After 40 iterations, the input is mostly sinusoidal except for truncation effects, see Fig. 6.
3) Interestingly, besides converging to a sinusoidal input signal that coincides with the worst-case signal in view of ℓ_2-induced norms, Procedure 2 also determines the

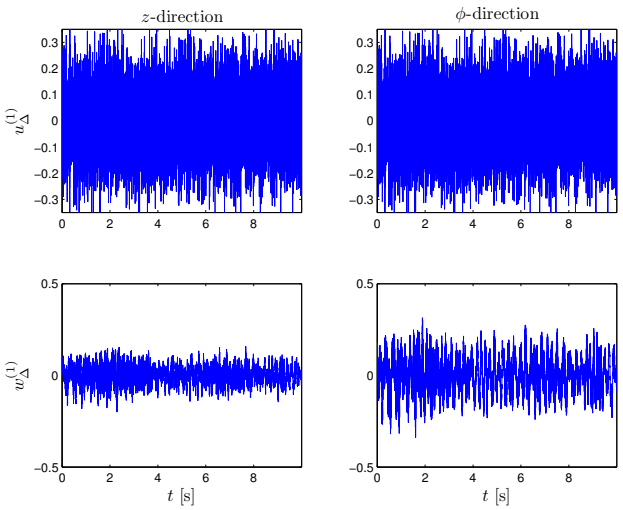

Fig. 5. Power iterations: iteration 1 of Procedure 2.

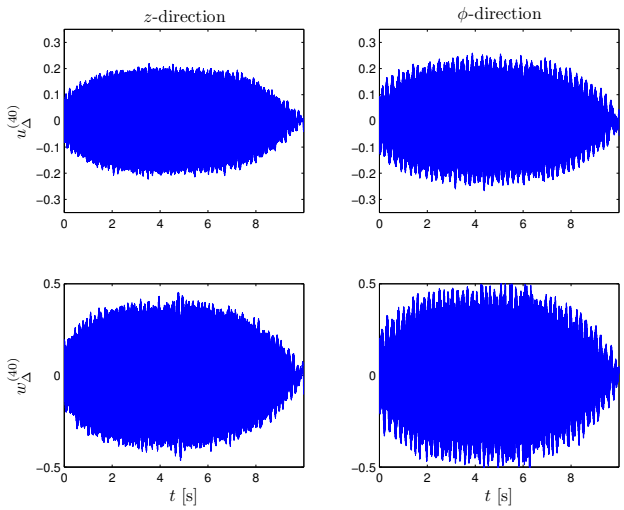

Fig. 6. Power iterations: iteration 40 of Procedure 2.

worst-case input direction. This is confirmed by the amplitudes of $\underline{u_\Delta}^{(40)}$ in both z-direction and ϕ-direction that have a comparable magnitude.

Next, estimator (12) is evaluated for all 40 iterations. The results are depicted in Fig. 7. This leads to the following observations.

1) the estimate $\hat{\gamma}_2^{(n)}$ seems to converge for increasing n. This leads to $\hat{\gamma}_2^{(40)} = 1.997$.
2) When comparing the estimated $\hat{\gamma}_2^{(40)} = 1.997$ with the result in Sec. IV-A, which is based on the frequency response function estimate in Fig. 4, it is observed that Procedure 2 leads to a higher value $\hat{\gamma}_2^{(40)}$ compared to $\sup_\omega \bar{\sigma}(\Delta_o)$. Interestingly, inspection of the input signal $u_\Delta^{(40)}$ reveals that the dominant frequency component is 121 [Hz], which differs significantly from the worst-case frequency of 296 [Hz] that is obtained in Sec. IV-A. Hence, Procedure 2 provides an effective means for determining the worst-case frequency in view of $\mathcal{H}_\infty$-norm estimation. In this application, it leads to more accurate results than a fixed pre-chosen frequency grid. In this respect, Procedure 2 is considered as an effective adaptive experiment design approach.

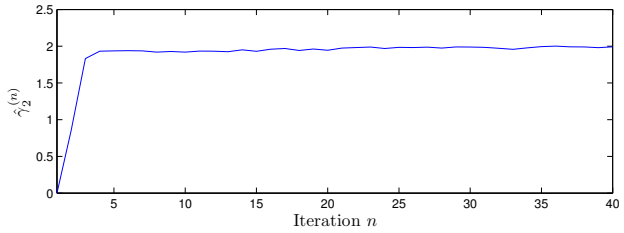

Fig. 7. Estimated norm $\hat{\gamma}_2^{(n)}$.

V. Discussion

A. A model error modeling perspective

As is experimentally shown in Sec. IV-B, Procedure 2 leads to a higher and hence more accurate estimation of the $\mathcal{H}_\infty$-norm compared to the use of an *a priori* chosen frequency grid, as is exemplified in Sec. IV-A and also done in, e.g., [16]. From this perspective, Procedure 2 can be seen as an adaptive experiment design procedure. As a result, Procedure 2 reduces estimation errors due to the use of a discrete frequency grid when compared to the uncertainty modeling procedure in [16]. From this perspective, it is emphasized that the use of *prior* assumptions to bound the interpolation error, as is done in, e.g., [20], [17], [21], is likely to lead to conservative results, as is also argued in [22, 9.5.2].

B. Connections to related (iterative) approaches

The approach presented in Sec. III is related to several identification and iterative control algorithms in the literature. For a connection to maximum likelihood estimation, see [8, Remark 10].

The iterative algorithm in Sec. III can be related to iterative learning control (ILC) algorithms [1]. For simplicity, consider the situation of Procedure 1, in which case the input during the next iteration is given by

$$\underline{u_\Delta}^{(n+1)} = \mathcal{T}_N \underline{w_\Delta}^{(n)}, \tag{14}$$

which closely resembles ILC update laws that are typically also a linear function of the signals $\underline{w_\Delta}^{(n)}$ and $\underline{u_\Delta}^{(n)}$. However, there are some principal differences when comparing typical ILC algorithms and Procedure 1. Hereto, assume as in Sec. III-C that an input normalization is implemented (this requires a small modification of estimators (6) and (12), see Sec. III-Cand [8]) as in (13), with $\mu^{(n+1)} = \|\underline{w_\Delta}^{(n)}\|_2$, i.e., the 2-norm of the input is normalized to 1. This leads to the input to the true system

$$\overline{\underline{u_\Delta}}^{(n+1)} = \frac{1}{\|\underline{w_\Delta}^{(n)}\|_2} \underline{u_\Delta}^{(n+1)} = \frac{1}{\|\underline{w_\Delta}^{(n)}\|_2} \mathcal{T}_N \underline{w_\Delta}^{(n)},$$

with output

$$\underline{w_\Delta}^{(n+1)} = \Delta_o \overline{\underline{u_\Delta}}^{(n+1)} = \Delta_o \frac{1}{\|\underline{w_\Delta}^{(n)}\|_2} \mathcal{T}_N \underline{w_\Delta}^{(n)}. \tag{15}$$

In (15), the operator $\Delta_o \frac{1}{\|\underline{w_\Delta}^{(n)}\|_2} \mathcal{T}_N$ maps $\mathbb{R}^N$ onto itself. Notice that the amplification of Δ_o for the input $\underline{w_\Delta}^{(n)}$ equals the 2-norm of the output $\underline{w_\Delta}^{(n+1)}$. Under mild assumptions, which is related to the comment in [8, Remark 9], $\|\underline{w_\Delta}^{(n+1)}\|_2 > \|\underline{w_\Delta}^{(n)}\|_2$. Since $\mathcal{T}$ has induced 2-norm equal to one, the induced 2-norm of $\Delta_o \frac{1}{\|\underline{w_\Delta}^{(n)}\|_2} \mathcal{T}_N$ is larger than one. As a result, (15) is a Lipschitz continuous function with Lipschitz constant larger than one, hence (15) is not a contraction. In contrast, ILC algorithms are also of the form (15), but designed such that the iteration (15) is a contraction map, corresponding to a Lipschitz constant that is strictly smaller than one. Such a contraction map ensures convergence to a unique fixed point, generally being an error signal of the system converging to zero.

The novel multivariable result of Procedure 2 provides further extensions to the implementation of ILC algorithms. In particular, in certain ILC algorithms referred to as adjoint ILC algorithms, see [23] and references therein, it is desired to filter through the transpose of the system. Clearly, the use of time reversal operators as in (4) enables a direct evaluation on the true system and effectively renders the need for a model in ILC algorithms superfluous. Interestingly, a slight modification of Procedure 2 directly enables its use for multivariable ILC algorithms that do not need a model of the system.

VI. Conclusion

In this paper, a novel data-driven $\mathcal{H}_\infty$-norm estimation procedure, which relies on iterative experiments on the system, is proposed for multivariable systems. This procedure is employed for model error modeling purposes. Experimental results of an active vibration isolation system show fast convergence of the algorithm and its ability to determine both the worst-case frequency and worst-case input and output directions in $\mathcal{H}_\infty$-norm estimation. The experimental results confirm that the iterative algorithm is useful for experiment design, i.e., to iteratively/adaptively determine improved inputs for $\mathcal{H}_\infty$-norm estimation, leading to improved results. Finally, in Sec. V-B, connections to related iterative learning algorithms are presented.

The result can be directly embedded in a system identification and robust control framework. Hereto, the resulting robust performance hinges on the choice of uncertainty structure, since the proposed iterative approach only delivers an $\mathcal{H}_\infty$-norm bound and not the commonly used weighting filters that shape the model error over frequency. By exploiting the freedom in model uncertainty structures, a non-conservative robust control design can be obtained by using the uncertainty structure in [24]. Although this uncertainty structure has been tacitly used in Sec. IV-B, details and subsequent robust control are beyond the scope of this paper.

The proposed results can be directly extended to other approaches. Besides a possible use in iterative learning control algorithms, see Sec. V-B, it can be directly used in any multivariable estimation problem that involves maximum eigenvalues. Finally, it is remarked that a full stochastic analysis of the multivariable situation, as is done in [8] for the SISO case, is beyond the scope of the present paper.

Acknowledgements

The authors would like to thank Okko Bosgra, Robbert van Herpen, and Bo Wahlberg for their contribution to this work.

References

[1] D. A. Bristow, M. Tharayil, and A. G. Alleyne, "A survey of iterative learning control: A learning-based method for high-performance tracking control," *IEEE Contr. Syst. Mag.*, vol. 26, no. 3, pp. 96–114, 2006.

[2] Z. Bien and J.-X. Xu, *Iterative Learning Control: Analysis, Design, Integration and Applications*. Norwell, MA, USA: Kluwer Academic Publishers, 1998.

[3] D. Gorinevsky, "Loop shaping for iterative control of batch processes," *IEEE Contr. Syst. Mag.*, vol. 22, no. 6, pp. 55–65, 2002.

[4] K. L. Moore, "Iterative learning control an expository overview," *Appl. Comp. Contr. Sign. Proc. Circ.*, vol. 1, pp. 151–214, 1999.

[5] P. Albertos and A. Sala, Eds., *Iterative Identification and Control*. London, UK: Springer, 2002.

[6] H. Hjalmarsson, "From experiment design to closed-loop control," *Automatica*, vol. 41, pp. 393–438, 2005.

[7] B. Wahlberg, M. Barenthin Syberg, and H. Hjalmarsson, "Non-parametric methods for $\mathcal{L}_2$-gain estimation using iterative experiments," *Automatica*, vol. 46, no. 8, pp. 1376–1381, 2010.

[8] C. R. Rojas, T. Oomen, H. Hjalmarsson, and B. Wahlberg, "Analyzing iterations in identification with application to nonparametric $\mathcal{H}_\infty$-norm estimation," *Automatica*, vol. 48, no. 11, pp. 2776–2790, 2012.

[9] M. Barenthin, M. Enqvist, B. Wahlberg, and H. Hjalmarsson, "Gain estimation for Hammerstein systems," in *14th IFAC Symp. Sys. Id.*, Newcastle, Australia, 2006, pp. 784–789.

[10] K. L. Moore, *Iterative Learning Control for Deterministic Systems*. London, UK: Springer-Verlag, 1993.

[11] R. Tousain, E. van der Meché, and O. Bosgra, "Design strategy for iterative learning control based on optimal control," in *Proc. 40th Conf. Dec. Contr.*, Orlando, FL, USA, 2001, pp. 4463–4468.

[12] G. H. Golub and C. F. Van Loan, *Matrix Computations*, 3rd ed. Baltimore, MD, USA: The John Hopkins University Press, 1996.

[13] D. Karnopp, "Active and semi-active vibration isolation," *Trans. ASME*, vol. 117, pp. 177–185, 1995.

[14] K. Zhou, J. C. Doyle, and K. Glover, *Robust and Optimal Control*. Upper Saddle River, NJ, USA: Prentice Hall, 1996.

[15] L. Ljung, "Model validation and model error modeling," in *The Åström Symposium on Control*, B. Wittenmark and A. Rantzer, Eds. Lund, Sweden: Studentlitteratur, 1999, pp. 15–42.

[16] M. van de Wal, G. van Baars, F. Sperling, and O. Bosgra, "Multivariable $\mathcal{H}_\infty/\mu$ feedback control design for high-precision wafer stage motion," *Contr. Eng. Prac.*, vol. 10, no. 7, pp. 739–755, 2002.

[17] D. K. de Vries and P. M. J. Van den Hof, "Quantification of model uncertainty from data," *Int. J. Rob. Nonlin. Contr.*, vol. 4, no. 2, pp. 301–319, 1994.

[18] T. Oomen, C. R. Rojas, H. Hjalmarsson, and B. Wahlberg, "Analyzing iterations in identification with application to nonparametric $\mathcal{H}_\infty$-norm estimation," in *IFAC 18th Triennial World Congress*, Milan, Italy, 2011, pp. 9972 – 9977.

[19] R. Pintelon and J. Schoukens, *System Identification: A Frequency Domain Approach*. New York, NY, USA: IEEE Press, 2001.

[20] A. J. Helmicki, C. A. Jacobson, and C. N. Nett, "Control oriented system identification: A worst-case/deterministic approach in $\mathcal{H}_\infty$," *IEEE Trans. Automat. Contr.*, vol. 36, no. 10, pp. 1163–1176, 1991.

[21] J. Chen and G. Gu, *Control-Oriented System Identification: An $\mathcal{H}_\infty$ Approach*. New York, NY, USA: John Wiley & Sons, 2000.

[22] G. Vinnicombe, *Uncertainty and Feedback: $\mathcal{H}_\infty$ loop-shaping and the ν-gap metric*. London, UK: Imperial College Press, 2001.

[23] J. D. Ratcliffe, J. J. Hätönen, P. L. Lewin, E. Rogers, and D. H. Owens, "Robustness analysis of an adjoint optimal iterative learning controller with experimental verification," *Int. J. Rob. Nonlin. Contr.*, vol. 18, no. 10, pp. 1089–1113, 2008.

[24] T. Oomen and O. Bosgra, "System identification for achieving robust performance," *Automatica*, vol. 48, no. 9, pp. 1975–1987, 2012.